CHEMISTRY
A EUROPEAN JOURNAL

COMMUNICATION

DOI: 10.1002/chem.201300592

Exclusive synthesis of $Au_{11}(PPh_3)_8Br_3$ against the Cl Analogue and the Electronic Interaction between Cluster Metal Core and Surface Ligands

Zhikun Wu*[a] and Rongchao Jin*[b]

The phosphine-protected Au_{11} cluster has attracted extensive interest for over four decades[1–12] due to its interesting properties and its use as a building block for large nanoclusters;[11,13] phosphine-protected Au_{13},[14] Au_9 and Au_{10}[15] have also been pursued recently. An interesting fact is that no solely phosphine-protected Au_{11} has been found, other negative ions or ligands always co-exist with phosphine, and the general formula of Au_{11} can be represented as $Au_{11}(PR_3)_7X_3$ (X = Cl, SCN, CN, SR, etc.). The structure of Au_{11} was revealed to be an incomplete icosahedral skeleton with an approximately C_{3v} symmetry by single crystal X-ray diffraction by various research groups.[1,2,10,12] Recently, it was found that the number of phosphine can be eight, too, when triphenyl phosphine was employed to protect the Au_{11} core,[9,11] and the formula was determined to be $Au_{11}(PPh_3)_8Cl_3$ by electrospray ionization mass spectrometry (ESI), thermogravimetric analysis (TGA), elemental analysis, etc. In both cases (i.e., $Au_{11}(PR_3)_7Cl_3$ and $Au_{11}(PPh_3)_8Cl_3$), the numbers of gold atoms and halogen atoms are constant (11 and 3, respectively) whereas the number of phosphine is slightly varied (from 7 to 8), which can be explained in terms of the closure of the electron shells created by spherical potentials.[16–18] Unlike another magic-size cluster Au_{25},[19–23] the synthesis of Au_{11} always starts from the Au^I precursor by a one-phase process. The synthesis from cheaper Au^{III} salt is not available in the literature, and the mechanism of the synthesis is still largely unclear. Other questions include: 1) is there some affinity competition when different halogen ions coexist in the synthesis system, and 2) can the metal core electrons interact with the benzene π electrons in triphenyl phosphine? The latter two issues are seemly not particularly relevant to one another, but both of them are closely related to the surface of Au_{11}. It has been revealed in our previous work that the surface can greatly influence the properties of gold nanoclusters.[24] To address these questions, we herein start from $HAuCl_4$ and have developed a two-phase protocol (tetraoctylammonium bromide (TOAB) as the phase transfer reagent) to synthesize Au_{11} clusters. Our experiments confirmed the applicability of two-phase synthesis for Au_{11}, and revealed that bromo-substituted Au_{11} is the exclusive product even if the Br/Cl ratio was 1:4 at the start, due to the thermodynamic stability difference. Furthermore, NMR spectroscopy and optical absorption spectroscopy identified the interaction between the cluster core electrons and the ligand's benzene π electrons.

Weare et al. previously synthesized $Au_{\sim 101}$ by a two-phase method (also using TOAB as the phase-transfer reagent) and proposed the intermediates, $Au(PPh_3)Cl$ and $O{=}PPh_3$, but without further identification.[25] Recently Goulet et al.[26] reported that, when the phase-transfer reagent (for instance: TOAB) was employed, the composition of the intermediate was different from the case without phase-transfer reagent; they identified the composition of the intermediate to be $[TOA][AuX_2]$ (X: halogen) by NMR spectroscopy in the Brust–Schiffrin synthesis.[26] Given that the size and dispersity of products of these syntheses are rather dependent upon the reaction conditions[20,21,27–29] and thus implicitly upon the reaction intermediates, it is important to establish clearly the composition of precursors to the final Au_{11} clusters during the reaction process. In the present work, the Au_{11} clusters are synthesized following a previously reported method of synthesizing Au_{25}[22] with modifications (for details, see the Experimental Section). First, the stoichiometry of the reduction of Au^{III} to Au^I by phosphine was established by direct observation of the solution color fading: when 1 equiv of PPh_3 (per mole of Au) was added, there was no sudden change of the solution color; after adding 1.87 equiv of PPh_3, the solution became turbid and the color faded obviously; further addition of 0.13 equiv of PPh_3 resulted in complete fading of the color of Au^{III} salt. UV/Vis monitoring also showed that the peak at 336 nm almost disappeared (Figure 1). The color change of the entire process is shown in Figure S1 in the Supporting Information.

The above titration experiments clearly show that the reduction process of Au^{III} to Au^I requires 2 equiv of PPh_3. To analyze the composition of the reaction intermediates, the precipitate and the solution were separated and analyzed. The precipitate cannot dissolve well in toluene, indicating

[a] Prof. Dr. Z. Wu
Key Laboratory of Materials Physics
Anhui Key Laboratory of Nanomaterials and Nanotechnology
Institute of Solid State Physics, Chinese Academy of Sciences
Hefei 230031 (P.R. China)
E-mail: zkwu@issp.ac.cn

[b] Prof. Dr. R. Jin
Department of Chemistry, Carnegie Mellon University
4400 Fifth Avenue, Pittsburgh, Pennsylvania 15213 (USA)
E-mail: rongchao@andrew.cmu.edu

Supporting information for this article is available on the WWW under http://dx.doi.org/10.1002/chem.201300592.

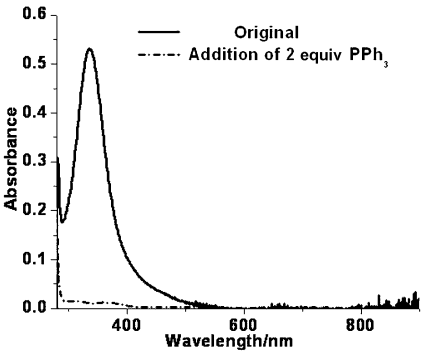

Figure 1. The UV/Vis spectra of Au^{III} solution after addition of 2 equiv of PPh_3 (the spectra were recorded immediately after the 0.3 μL reaction solution was diluted in 600 μL toluene).

that it may be the Au^I complex without the TOA^+ unit; NMR spectroscopy indeed confirmed this (i.e., no TOA^+ signals were found in the high-field region, Figure 2).

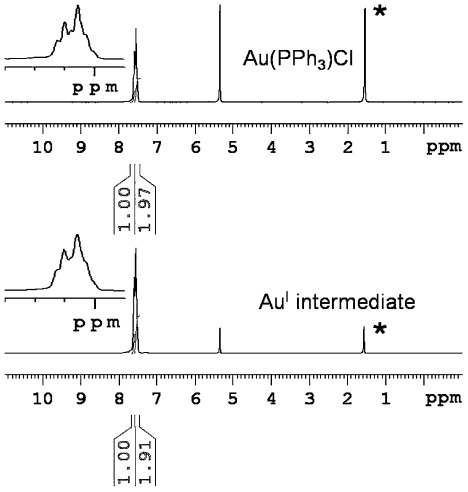

Figure 2. Comparison of the NMR spectra of the Au^I intermediate (bottom) and $Au(PPh_3)Cl$ (top; $CDCl_2$ as the solvent). The asterisks indicate the residual water in the NMR samples. The spike at 5.35 ppm is a residual solvent (CD_2Cl_2) peak. Insets: the enlargements of the portions corresponding to the benzene proton signals.

^1H NMR spectroscopy also showed the intermediate to be very similar to the standard spectrum of $Au(PPh_3)Cl$ (> 98%, from Strem Chemicals). Considering that the ligand in $Au(PPh_3)X$ may be Br^- (introduced by the phase-transfer reagent, TOAB), we performed thermogravimetric analysis (TGA) to find out whether Br or Cl is associated with the Au^I intermediate. We conducted three measurements and the losses of weight were 62.3, 62.3, and 62.2%, respectively (see Figure S2 for a typical TGA profile). The average loss of weight (62.3%) actually does not match the composition of $AuPPh_3Cl$ (expected loss: 60.2%), but is closer to the composition of $Au(PPh_3)Br$ (expected loss: 63.5%). The TGA result indicates that the Au^I intermediate in our case is mainly $Au(PPh_3)Br$. Indeed, laser desorption ionization (LDI) mass spectrometry confirms this (Figure S3 in the Supporting Information). On the other hand, NMR spectroscopy reveals that the main compounds left in the solution of the intermediate product are $OPPh_3$ and $[N(C_8H_{17})_4]^+$ (i.e., TOA^+). The peaks in the range of 7.4–7.8 ppm are the typical benzene proton signals of $OPPh_3$, and the proton number ratio in *o*-, *m*-, *p*-positions of benzene is 2:2:1 as expected (Figure S4 in the Supporting Information); for comparison, the standard NMR spectrum of $OPPh_3$ is also shown in Figure S4 in the Supporting Information. In the high-field region (0.8–3.5 ppm), all peaks can be assigned to TOA^+; specifically, the single peak at approximately 0.9 ppm is from the methyl group of TOA^+; the peak at about 3.3 ppm is from the methylene protons close to nitrogen ($-N(CH_2)-$); the peaks at approximately 1.7 ppm are assigned to the β-methylene protons (the position relative to N, $-NCH_2(CH_2)-$); the multiple peaks centered at about 1.3 ppm are assigned to the other methylene protons ($-NCH_2CH_2(CH_2CH_2CH_2CH_2CH_2)-$), and their number ratio based on the integrated areas is 4.72:2.79:2.96:15.53 (equal to 3.0:1.8:1.9:10.0), very close to the theoretical value 3:2:2:10. ESI-MS analysis further confirmed this: the peak at *m*/*z* 279.2 was assigned to $[OPPh_3+H]^+$ ($C_{18}H_{16}OP$, expected: 279.1), and the dominant peak at *m*/*z* 466.6 was assigned to $[TOA]^+$ ($C_{32}H_{68}N$, expected: 466.5); the isotope patterns match with the simulations well (Figure S5 in the Supporting Information).

Based on the above results, the reaction from Au^{III} to Au^I can be represented as follows [Eq. (1)]:

$$HAuCl_4 + 2\,PPh_3 + TOAB + H_2O \rightarrow Au(PPh_3)Br + OPPh_3 + TOAC + 3\,HCl \quad (1)$$

Our result is contrary to the case of Au^{III}/thiol system,[26] also different from the previous assumption of $Au(PPh_3)Cl$.[25]

In the present two-phase synthesis of Au_{11}, an interesting issue is the potential competition between Br^- and Cl^-. As mentioned above, the Au^I intermediate is mainly the bromide complex, rather than the chloride complex as expected, although Cl^- is far more in excess than Br^- under our reaction conditions. Furthermore, we found that Br^- is exclusively present in the final Au_{11} clusters as shown in the ESI mass spectrometric analysis (Figure 3). The dominant peak at *m*/*z* 4424.15 corresponds to the formula of $[Au_{11}(PPh_3)_8Br_2]^+$ ($Au_{11}Br_2C_{144}H_{120}P_8$, expected *m*/*z* 4424.21). In the lower *m*/*z* region, no obvious Cl substitute(s) was found in the ESI spectrum (note: for monosubstituted $Au_{11}(PPh_3)_8BrCl$, the expected molecular weight would be 4380.25, and for bisubstituted $Au_{11}(PPh_3)_8Cl_2$, the expected molecular weight would be 4335.30). Since the ESI spectrum was obtained in the positive mode, the full molecular formula of the dominant species should be $[Au_{11}(PPh_3)_8Br_3]$ (counterion: Br^-). TGA also confirmed this formula (Figure S6 in the Supporting Information): the observed weight loss (52.5%) is very close to the theoretical value of 51.9%.

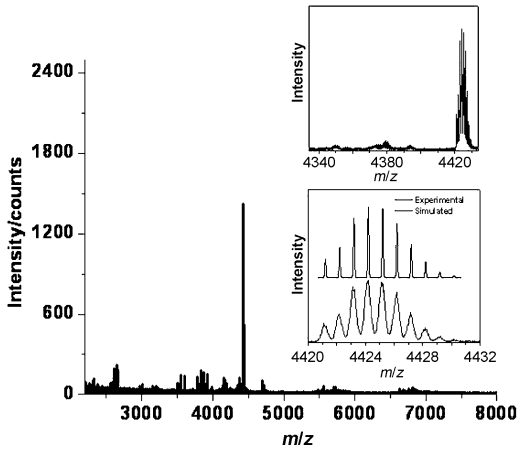

Figure 3. ESI mass spectrum of $Au_{11}(PPh_3)_8Br_3$. Top inset: the spectral section in the m/z range of 4334–4434; bottom inset: comparison of the simulated and experimental isotope patterns.

Here, an interesting question naturally arises—what makes $Au_{11}(PPh_3)_8Br_3$ the exclusive product even if the Br^-/Cl^- atom number ratio is 1:4 (see the Experimental Section)? Is it due to the kinetic control or thermodynamic stability?[30] As is known, Br^- is larger than Cl^- and the concentration of Br^- is much lower than that of Cl^-, so the kinetic consideration is not favored for the exclusive formation of $Au_{11}(PPh_3)_8Br_3$. Thus, the possible reason may be due to the thermodynamic stability difference; our further experiments confirmed this.

For comparison, we prepared $Au_{11}(PPh_3)_8Cl_3$ clusters (see the Experimental Section). To compare the stability, we monitored the intensity change of the 421 nm absorption peak of the $Au_{11}(PPh_3)_8Br_3$ and $Au_{11}(PPh_3)_8Cl_3$ under the same conditions (Figure S7 in the Supporting Information). At the start, both of them have the same absorption at 421 nm (0.22 OD, Figure S8 in the Supporting Information). After 13 min exposure to air and room light, the 421 nm absorption of $Au_{11}(PPh_3)_8Cl_3$ solution decreased rapidly to 0.14 OD, whereas for $Au_{11}(PPh_3)_8Br_3$ the peak intensity decrease was slower (to 0.19 OD only). After 4 h, the absorption of $Au_{11}(PPh_3)_8Cl_3$ solution at 421 nm decreased to 0.037 OD; in contrast, it took about 7 h for $Au_{11}(PPh_3)_8Br_3$ to decrease to the same absorption intensity. The decrease of absorption is due to the irreversible aggregation of Au_{11} clusters, which can be visually seen on the tube wall (Figure S9 in the Supporting Information). The slower aggregation rate of $Au_{11}(PPh_3)_8Br_3$ than $Au_{11}(PPh_3)_8Br_3$ indicates the enhanced stability of $Au_{11}(PPh_3)_8Br_3$ compared with $Au_{11}(PPh_3)_8Cl_3$.

It is known that some nanoclusters can be regarded as superatoms or analogues;[16–18] for $Au_{11}(PPh_3)_8Br_3$, it is an 8-electron ($n^* = Nv_A - M - Z = 11 - 2 - 1 = 8$; see ref. [17]) shell closing structure; that is, eight free-valence electrons of Au 6s are contained in the core consisting of eleven gold atoms. An essential question is: can the Au_{11} metal core electrons interact with the adjacent benzene π electrons? Our recent findings that ligands greatly influence the cluster chirality[22] and fluorescence[24a] imply this possibility. Herein NMR spectroscopy was employed for further investigation. NMR spectra revealed that the benzene protons in Au_{11} were shifted to high field (6.6 ppm), and the three subgroups (*o*-, *m*-, *p*-positions) of benzene signals were separated clearly (from 6.6 to 7.5 ppm) compared with the free ligands (essentially one broad peak centered at 7.37 ppm; Figure 4). In

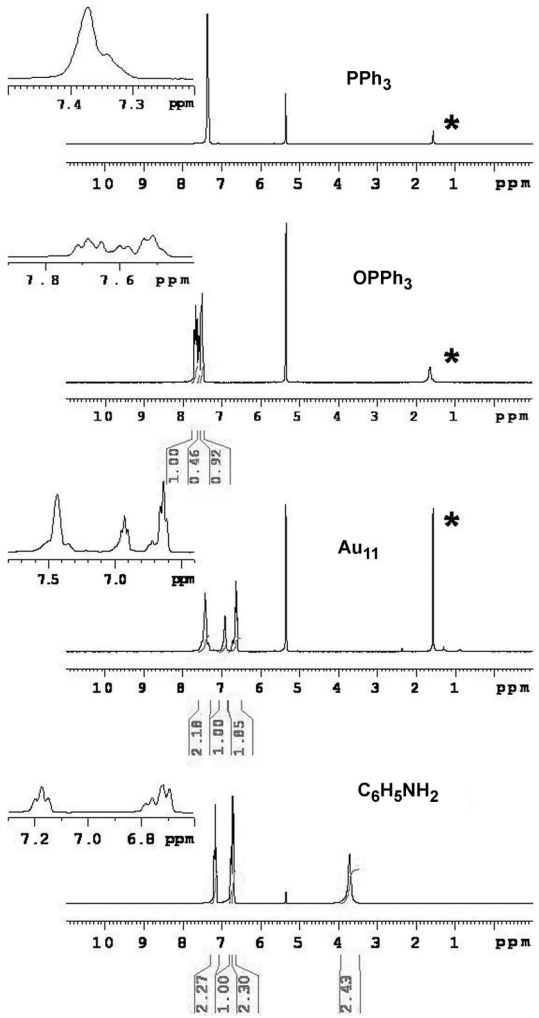

Figure 4. Comparison of the NMR spectra of the four materials. The asterisks indicate the residual water in the NMR samples. The spike at 5.35 ppm is a residual solvent (CD_2Cl_2) peak.

contrast, in phenylethanethiol-capped Au_{25}, not only the chemical shifts but also the spacings of different subgroup proton signals are similar to free ligand (Figure S10 in the Supporting Information). Therefore, the benzene protons in $Au_{11}(PPh_3)_8Br_3$ are more intimately coupled to the metal core than in $[Au_{25}(SCH_2CH_2Ph)_{18}]^-$ nanoclusters. It should be noted that Au_{25} is also an 8-electron shell closing structure. In the NMR spectrum of $Au_{11}(PPh_3)_8Br_3$, the benzene proton signals shifting to high field generally means an increase in delocalized electron density in benzene due to conjugation with the Au_{11} core; for example, the strong electron-donating group NH_2 in aniline can cause the benzene

proton signals to shift to higher field (6.7–7.2 ppm); in contrast, in $OPPh_3$ with an electron-withdrawing group (i.e., the oxygen atom), the benzene proton signals shift to lower field (7.5–7.7 ppm; Figure 4). In $Au_{11}(PPh_3)_8Br_3$, since the benzene ring is close to the metal core and the core is electron-rich, it is possible for the metal core electrons to conjugate with the benzene π electrons.

It is surprising to find that in $Au_{11}(PPh_3)_8Br_3$ the *m*- and *p*-position proton signals of the benzene ring shift to high field, whereas the *o*-position protons are not much influenced compared with that of free PPh_3 ligands (thus, resulting in enlargement of the spacings of three subgroup proton signals). This observation is distinctively different from the common aromatic compounds with electron-donating group(s), like aniline. The *o*-, *m*-, *p*-position proton assignment can be assisted with 2D COSY (Figure 5). To simplify

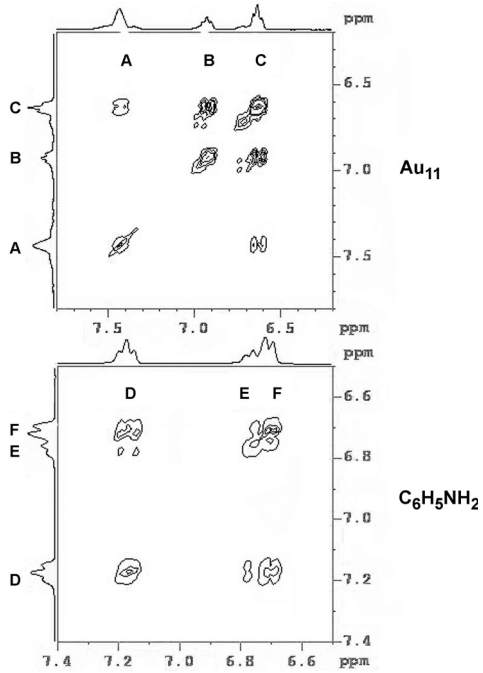

Figure 5. Comparison of the $^1H,^1H$ correlation spectra (COSY) of $Au_{11}(PPh_3)_8Br_3$ and $C_6H_5NH_2$.

the interpretation, the three subgroups of protons in $Au_{11}(PPh_3)_8Br_3$ are designated as A, B and C from low field to high field, respectively; for aniline, the three subgroups of protons are represented with D, E and F. From 1D spectra (Figure 5), based on the integrated area, the proton number ratio A/B/C is 2:1:2; thus it is clear that B represents the *p*-position proton since there is only one *p*-position proton. In 2D COSY (Figure 5), it can be found that C protons couple with A and B protons, so C protons should be the *m*-position protons since the *m*-position protons are adjacent to both *o*- and *p*-position protons. As a result, the remaining A should represent the *o*-position protons. Herein, the *m*-position protons in benzene of $Au_{11}(PPh_3)_8Br_3$ are located in the highest field (i.e., 6.6 ppm), which is contrary to the case of aniline, in which the *o*-position protons are located in the highest field (i.e., 6.7 ppm), and the *m*-position protons are located in the lowest field (Figure 4 and Figure 5), which can be understood since the amine group can influence the *o*-position electrons more than the *p*-position electrons. This difference (i.e., the relative chemical shifts in *o*- and *m*-positions in substituted benzene) between $Au_{11}(PPh_3)_8Br_3$ and aniline may be due to the different conjugation mechanism; in aniline, it is a p–π-type conjugation, whereas in $Au_{11}(PPh_3)_8Br_3$ it is a conjugation between the benzene π electrons and metal core electrons, which has not been reported previously. UV/Vis spectra provide further evidence for the conjugation between the metal core electrons and the benzene π electrons (Figure 6): the absorption peak associated with the PPh_3 unit red-shifts from approximately 265 nm in free PPh_3 to about 300 nm in $Au_{11}(PPh_3)_8Br_3$.

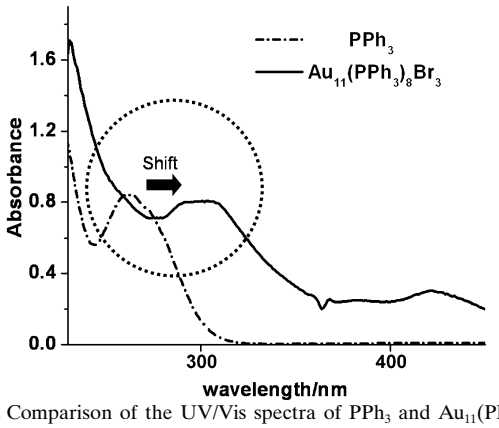

Figure 6. Comparison of the UV/Vis spectra of PPh_3 and $Au_{11}(PPh_3)_8Br_3$ (both dissolved in CH_2Cl_2).

In summary, we have developed a two-phase synthesis of monodisperse Au_{11} clusters with the precise composition determined to be $Au_{11}(PPh_3)_8Br_3$, and we have investigated the reaction intermediates by NMR spectroscopy, MS, TGA, etc. We found that Br^-, instead of Cl^-, was the dominant halogen in both the Au^I intermediate and the final Au_{11} product, although Cl^- was in large excess ($Br^-/Cl^- = 1:4$, molar ratio) and would kinetically favor binding with gold. Our result is explained by the finding that Br^- can enhance the stability of the cluster. Another interesting finding is the interaction of Au_{11} metal core electrons with benzene's π electrons probed by NMR and UV/Vis spectroscopy. We hope this work stimulates more research on the important issues related to nanocluster surface properties.

Experimental Section

Synthesis of Au_{11} clusters: Gold salt ($HAuCl_4 \cdot 3H_2O$, 224.9 mg, 0.57 mmol) was first dissolved in ethanol (0.5 mL), then tetraoctylammonium bromide (TOAB, 312.0 mg, 0.57 mmol) was added, followed by slow addition of toluene (9.6 mL) into the ethanol solution. The resulting mixture was stirred at a medium speed for about 15 min until the solution became unturbid, then the solution was cooled to approximately 0 °C in

an ice-bath over a period of 30 min. Triphenylphosphine (PPh_3, 300.2 mg, 1.14 mmol, dissolved in 4.7 mL toluene) was slowly added to the reaction mixture under slow stirring (~60 rpm). After the addition of PPh_3, the solution color faded quickly; further stirring for 2 h ensured the completion of the reaction. A freshly made, aqueous solution of $NaBH_4$ (260.5 mg, 6.9 mmol, dissolved in 7.1 mL ice-cold H_2O) was added rapidly into the reaction mixture under vigorous stirring. The solution was continuously stirred for approximately 40 h (note: in our previous work,[21,22] we found the aging time markedly influenced the purity and yield of clusters). For postsynthetic treatment, the water layer was first removed, and the remaining mixture was washed with Nanopure water twice; then the black precipitate was collected and thoroughly washed with toluene, recrystallized in CH_2Cl_2/hexane system several times, and UV/Vis and NMR spectroscopy were used to monitor the purity of the product. A small fraction of Au_{11} can also be isolated from the combined washing toluene solution. The as-prepared cluster was identified to be $Au_{11}(PPh_3)_8Br_3$. For the $Au_{11}(PPh_3)_8Cl_3$ synthesis, all the conditions were the same except that TOAB was replaced by TOAC (286.0 mg, 0.57 mmol).

For the investigation of the reaction intermediates the protocol was the same as above, except that the triphenylphosphine was added in three portions successively (the amounts were 1.0, 0.87 and 0.13 equiv, respectively; see illustration in Figure S1) with 1 h intervals to ensure the reaction was completed. After the addition of 2 equiv PPh_3 (total) and further stirring for two more hours, the solution was concentrated, and the white precipitate (mainly $Au(PPh_3)Br$, see the above discussion) was collected, thoroughly washed with toluene and MeOH, then dried for characterization. The remaining toluene solution was combined with all the filtrate and was dried under reduced pressure for further purification.

Characterization: UV/Vis absorption spectra were recorded in the range 190–1100 nm by using a Hewlett–Packard (HP) 8543 diode array spectrophotometer. Laser desorption ionization (i.e., no matrix) mass spectrometry analyses were performed with a PerSeptive Biosystems Voyager DE super-STR time-of-flight (TOF) mass spectrometer. Electrospray ionization mass spectra were acquired by using a quadrupole field ion trap mass spectrometer (for $OPPh_3$ and TOA^+ identification, MeOH as solvent) or a Waters Q-TOF mass spectrometer equipped with Z-spray source (for Au_{11} identification, 1:1 v/v CH_2Cl_2/MeOH as solvent). NMR analysis was conducted on a Bruker Avance™ DMX 500 spectrometer by using standard Bruker software. The data were collected with samples dissolved in CD_2Cl_2. The NMR peak assignments were made by the following experiments: 1D ^1H NMR spectroscopy, ^1H,^1H correlation spectroscopy (COSY). Thermogravimetric analysis (TGA) was carried out on a TG/DTA6300 thermogravimetric analyzer (Seiko Instruments, Inc.) with a 5 °C min^{-1} heating rate and an approximately 50 mL min^{-1} N_2 flow-rate. About 2.0 mg of fine solid samples were used in TGA.

Acknowledgements

Z.W. thanks the support by "Hundred Talents Program" of the Chinese Academy of Sciences, National Basic Research Program of China (Grant No. 2013CB934302), the Natural Science Foundation of China (Grant No. 21222301, 21171170) and startup from the Ministry of Human Resources and Social Security of China. R.J. acknowledges the support by Air Force Office of Scientific Research under AFOSR Award No. FA9550-11-1-9999 (FA9550-11-1-0147) and the Camille Dreyfus Teacher-Scholar Awards Program.

Keywords: conjugation · gold · nanoclusters · phosphane ligands · synthetic methods

[1] V. G. Albano, P. L. Bellon, M. Manassero, M. Sansoni, *J. Chem. Soc. Chem. Commun.* **1970**, 1210.
[2] P. Bellon, M. Manassero, M. Sansoni, *J. Chem. Soc. Dalton Trans.* **1972**, 1481.
[3] F. Cariati, L. Naldini, *Inorg. Chim. Acta* **1971**, *5*, 172.
[4] P. A. Bartlett, B. Bauer, S. J. Singer, *J. Am. Chem. Soc.* **1978**, *100*, 5085.
[5] F. A. Vollenbroek, J. J. Bour, J. M. Trooster, J. W. A. van der Velden, *J. Chem. Soc. Chem. Commun.* **1978**, 907.
[6] F. A. Vollenbroek, W. B. P. Bosman, J. J. Bour, J. H. Noordik, P. T. Beurskens, *J. Chem. Soc. Chem. Commun.* **1979**, 387.
[7] F. A. Vollenbroek, J. P. Berg, J. W. A. van der Velden, J. J. Bour, *Inorg. Chem.* **1980**, *19*, 2685.
[8] R. C. B. Copley, D. M. P. Mingos, *J. Chem. Soc. Dalton Trans.* **1996**, 479.
[9] G. H. Woehrle, M. G. Warner, J. E. Hutchison, *J. Phys. Chem. B* **2002**, *106*, 9979.
[10] K. Nunokawa, S. Onaka, T. Yamaguchi, T. Ito, S. Watase, M. Nakamoto, *Bull. Chem. Soc. Jpn.* **2003**, *76*, 1601.
[11] Y. Shichibu, Y. Negishi, T. Tsukuda, T. Teranishi, *J. Am. Chem. Soc.* **2005**, *127*, 13464.
[12] K. Nunokawa, S. Onaka, M. Ito, M. Horibe, T. Yonezawa, H. Nishihara, T. Ozeki, H. Chiba, S. Watase, M. Nakamoto, *J. Organomet. Chem.* **2006**, *691*, 638.
[13] K. Nunokawa, S. Onaka, Y. Mizuno, K. Okazaki, T. Sunahara, M. Ito, M. Yaguchi, H. Imai, K. Inoue, T. Ozeki, H. Chiba, T. Yoshida, *J. Organomet. Chem.* **2005**, *690*, 48.
[14] Y. Shichibu, K. Konishi, *Small* **2010**, *6*, 1216.
[15] J. M. Pettibone, J. W. Hudgens, *ACS Nano* **2011**, *5*, 2989.
[16] W. D. Knight, K. Clemenger, W. A. de Heer, W. A. Saunders, M. Y. Chou, M. L. Cohen, *Phys. Rev. Lett.* **1984**, *52*, 2141.
[17] M. Walter, J. Akola, O. Lopez-Acevedo, P. D. Jadzinsky, G. Calero, C. J. Ackerson, R. L. Whetten, H. Gronbeck, H. Hakkinen, *Proc. Natl. Acad. Sci. USA* **2008**, *105*, 9157.
[18] Z. Wu, R. Jin, *Chem. Eur. J.* **2011**, *17*, 13966.
[19] R. L. Donkers, D. Lee, R. W. Murray, *Langmuir* **2004**, *20*, 1945.
[20] M. Zhu, E. Lanni, N. Garg, M. E. Bier, R. Jin, *J. Am. Chem. Soc.* **2008**, *130*, 1138.
[21] Z. Wu, J. Suhan, R. Jin, *J. Mater. Chem.* **2009**, *19*, 622.
[22] Z. Wu, C. Gayathri, R. R. Gil, R. Jin, *J. Am. Chem. Soc.* **2009**, *131*, 6535.
[23] Z. Wu, R. Jin, *ACS Nano* **2009**, *3*, 2036.
[24] a) Z. Wu, R. Jin, *Nano. Lett.* **2010**, *10*, 2568; b) Z. Wu, M. Wang, J. Yang, X. Zheng, W. Cai, G. Meng, H. Qian, H. Wang, R. Jin, *Small* **2012**, *8*, 2028; c) M. Wang, Z. Wu, J. Yang, G. Wang, H. Wang, W. Cai, *Nanoscle* **2012**, 4, 2087; d) Z. Wu, *Angew. Chem.* **2012**, *124*, 2988; *Angew. Chem. Int. Ed.* **2012**, *51*, 2934.
[25] W. W. Weare, S. M. Reed, M. G. Warner, J. E. Hutchison, *J. Am. Chem. Soc.* **2000**, *122*, 12890.
[26] P. J. G. Goulet, R. B. Lennox, *J. Am. Chem. Soc.* **2010**, *132*, 9582.
[27] M. Brust, M. Walker, D. Bethell, D. J. Schiffrin, R. Whyman, *J. Chem. Soc. Chem. Commun.* **1994**, 801.
[28] D. Leff, P. C. Ohara, J. R. Heath, W. M. Gelbart, *J. Phys. Chem.* **1995**, *99*, 7036.
[29] M. J. Hostetler, J. E. Wingate, C.-J. Zhong, J. E. Harris, R. W. Vachet, M. R. Clark, J. D. Londono, S. J. Green, J. J. Stokes, G. D. Wignall, G. L. Glish, M. D. Porter, N. D. Evans, R. W. Murray, *Langmuir* **1998**, *14*, 17.
[30] Z. Wu, M. A. MacDonald, J. Chen, P. Zhang, R. Jin, *J. Am. Chem. Soc.* **2011**, *133*, 9670.

Received: February 15, 2013
Revised: June 5, 2013
Published online: August 13, 2013

